Acta Geodyn. Geomater., Vol. 18, No. 2 (202), 199–208, 2021
DOI: 10.13168/AGG.2021.0014
journal homepage: https://www.irsm.cas.cz/acta

ORIGINAL PAPER

DISTRIBUTION OF METALLOGENIC ZONES OF THE CAUCASUS REGION ORIGINATED AS A RESULT OF THE SUBDUCTION OF THE LITHOSPHERE OF THE TETHYS PALEO-OCEANIC PLATE UNDER THE EAST-EUROPEAN PALEO-CONTINENTAL PLATE

Andrey Leonidovich KHARITONOV [1] *and Sergey Vladilenovich GAVRILOV [2]

[1] *Pushkov Institute of Terrestrial Magnetism, Ionosphere and Radio Wave Propagation of RAS, Moscow, 4, Kaluzhskoe Highway, Russia*
[2] *Schmidt Institute of Physics of the Earth of RAS, Moscow, 10, Bolshaya Gruzinskaya, Russia*

**Corresponding author's e-mail:* haritonov-magnit@yandex.ru

ARTICLE INFO

Article history:
Received 20 January 2021
Accepted 26 March 2021
Available online 18 April 2021

Keywords:
Subduction velocity of Tethys paleo-oceanic lithospheric plate
Karig-Richter convective flows
Mantle wedge thermal convection
Mantle rheology
Calc-alkali magmas
Metallogenic zones

ABSTRACT

On the assumption that the 2D heat flux anomaly in the territory of Caucasus is provided by the convective heat transfer from the mantle wedge, the angle and velocity of subduction of the paleo-lithospheric plate Tethys (Mediterranean and East Black Sea paleo-lithospheric plates) under the East-European paleo-lithospheric plate (Caucasus region) are estimated numerically. Within the framework of the geodynamical model constructed the horizontal extent of the 2D heat flux anomaly observed in the rear of the Caucasus mountain belt corresponds to subduction velocity of ~ 40 mm per year which is close to that observed with the help of geodetic means. The upwelling convective mantle flows can transport the mantle calc-alkali magmas (containing metals) to the subsurface Earth's crust layers, thus making the ore deposits to be attached to the upper lithospheric locations above the ascending flows of the Karig-Richter vortices.

INTRODUCTION

The problem of origin of metallogenic provinces is discussed by the number of American scientists (Noble, 1970; Karig, 1971; Sillitoe, 1972; Condie, 1976; Hirth et al., 2003). Some geologists (Noble, 1970; Sillitoe, 1972; Fercshtatter, 2012) regard the spatial distribution of the metallogenic provinces (or the metallogenic zones) as reflecting the heterogeneities in the distribution of metals in the upper mantle (Fig. 1).

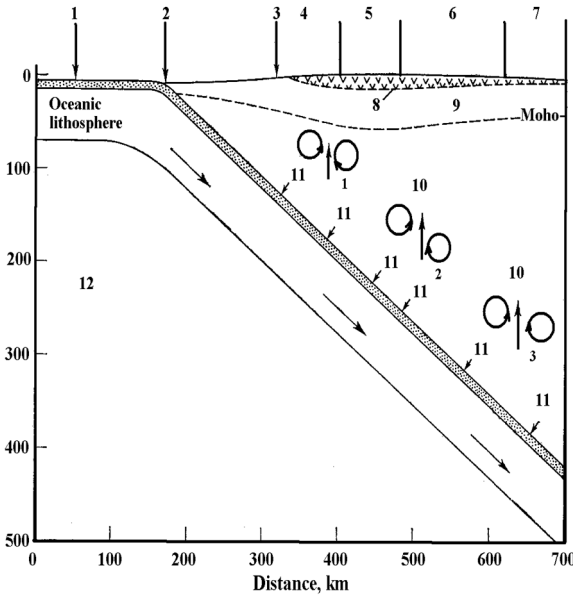

Fig. 1 Schematic vertical cross-section of a typical subduction zone showing the surface distribution of the metallogenic provinces (4-7) above the some pairs of the convective Karig-Richter vortices (10) over the subducting slab (Karig, 1971). The metals-containing calc-alkali magmas entrained in the upwelling mantle flows (shown by vertical arrows) provide the formation of the subsurface ore deposits in the Earth's crust (Sillitoe, 1972). 1 – oceanic crust and lithosphere; 2 – oceanic trench; 3 – coast of the continental lithospheric plate; 4 – zone of accumulation of iron-containing ores; 5 – zone of accumulation of ores containing gold (Au) and copper (Cu); 6 - zone of accumulation of ores containing silver (Ag), lead (Pb), zinc (Zn); 7 - zone of accumulation of ores containing tin (Sn), molybdenum (Mo); 8 - sedimentary layer; 9 - zone of calc-alkali intrusions and volcanic rocks; 10 - zone of rise of calc-alkali magmas and metals contained in them; 11 - partial melting in the absorption zone of oceanic crust layers and metals contained therein; 12 –the asthenosphere.

Cite this article as: Kharitonov AL, Gavrilov SV: Distribution of metallogenic zones of the Caucasus region originated as a result of the subduction of the lithosphere of the Tethys Paleo-Oceanic plate under the East-European Paleo-Continental plate. Acta Geodyn. Geomater., 18, No. 2 (202), 199–208, 2021. DOI: 10.13168/AGG.2021.0014

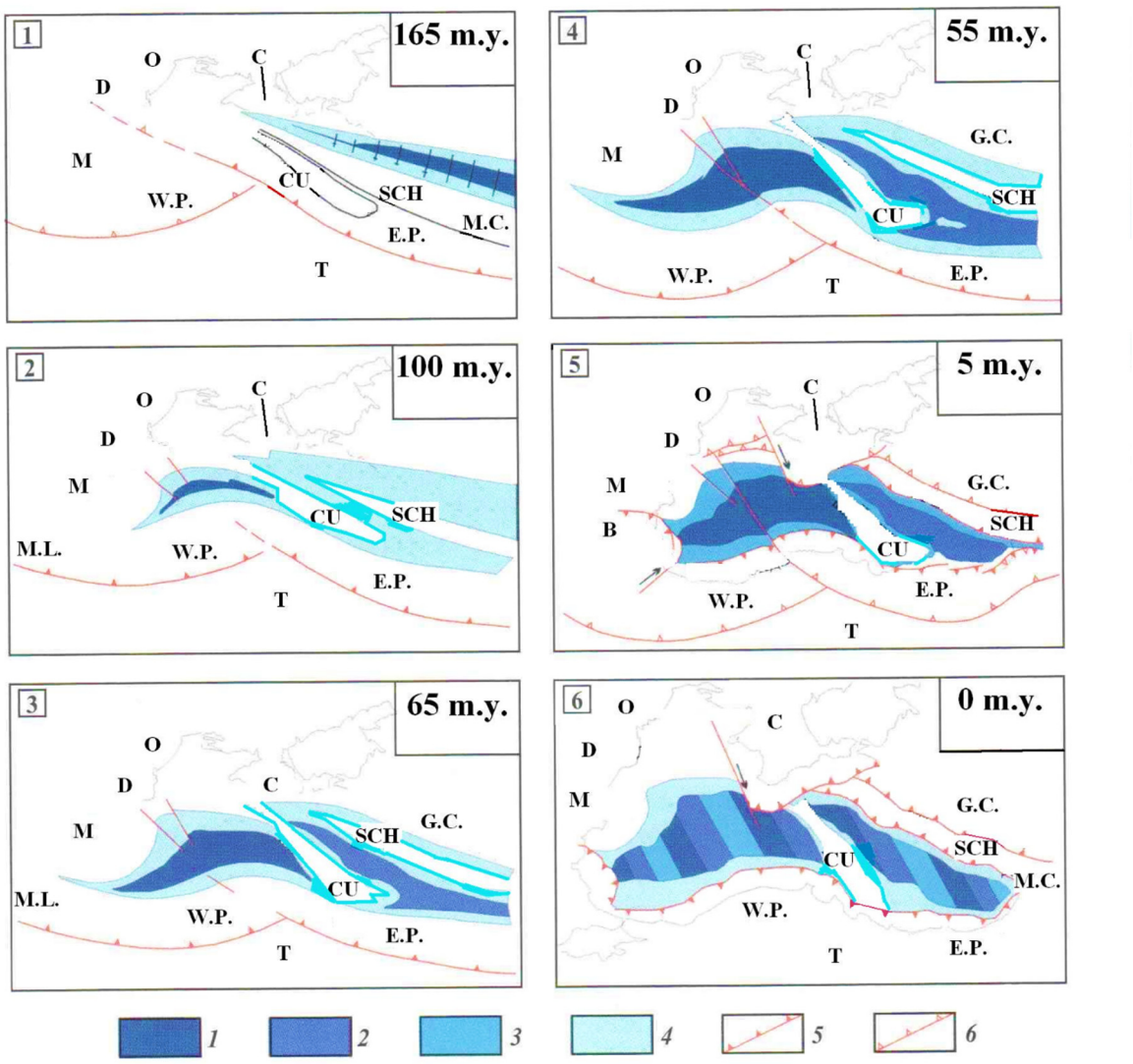

Fig. 2 Geodynamic evolution of the Tethys paleo-oceanic plate (Black Sea basin) in the Mesozoic-Cenozoic geological and chronological period (165 m.y. – 0 m.y.) according to (Finetti, 1988; Glumov et al., 2014). Maps in Figure 2: № 1 – the end of the Middle Jurassic geological period (165 m.y.); № 2 – the end of the Early Cretaceous geological period (100 m.y.); № 3 – the end of the Late Cretaceous geological period (65 m.y.); № 4 – the end of the Late Paleocene geological period (55 m.y.); № 5 – the end of the Late Miocene geological period (5 m.y.); № 6 - (0 m.y.); 1 - oceanic crust; 2 – highly thinned continental crust; 3 – zone of ancient crust conservation; 4 - back– arc basins and continental margins; 5 – active subduction zones; 6 - zones of subduction slope; O – the Odessa monocline; M – the Myzian paleo-platform; D – the Dobrudja region; M.L. - the Midlands; B – the Balcan region; C – the Cremean region; G.C. – the Great Caucasus region; M.C. – the Minor Caucasus (Dzirula) region; CU – the Archangelsky orogenic uplift; SCH – the Schatsky orogenic uplift; W.P. – the Western Pontides; E.P. – the Eastern Pontides; T – the Tethys paleo-oceanic plate.

With the help of geological data in (Isacks et al., 1968; Noble, 1970; Sillitoe, 1972; Condie, 1976; Glumov et al., 2014) the necessary changes in the geodynamic structure of the East Black Sea (and Mediterranean) lithosphere having taken place in the course of the Earth's evolutionary development (since 165 m.y. ago till now) can be shown to result in the gradual formation of basic tectonic structures, i.e. the Schatsky shaft-like orogenic uplift and its continuation (the Minor Caucasus ridge and parallel Great Caucasus ridge and corresponding depression in between) in the eastern sector (Eastern Pontides) of the paleo-oceanic lithospheric plate of the ancient Tethys ocean (1). The latter plate comprised the East Black Sea plate as well as the shaft-like orogenic structures of the Great and Minor Caucasus, which were gradually subducting (№ 1 – № 6) under the East-European paleo-lithospheric plate, the leading region of the Great Caucasus having been subject to compressive stresses (Fig. 2).

The goal of the present paper is to attempt the plate tectonic explanation of the origin of metallogenic

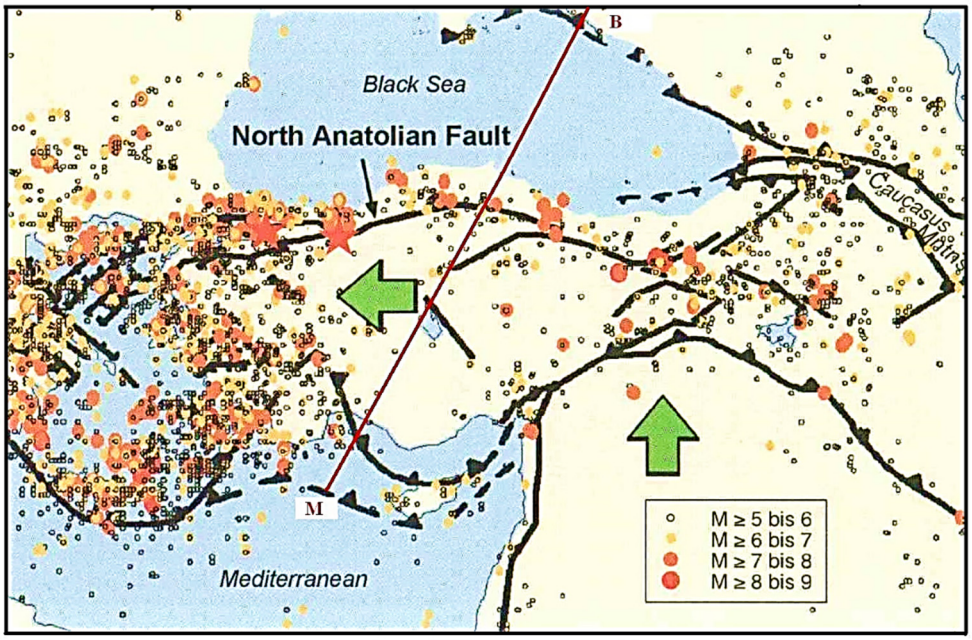

Fig. 3 Map of the present-day location Mediterranean-East Black Sea subduction zone and hypocenters of earthquakes of this region. MB – the profile of the geodynamic model of the Mediterranean-East Black Sea subduction zone.

provinces in the Caucasus region. According to Glumov et al. (2014), the interaction of lithospheric plates in the East Black Sea region lead to gradual subduction of the East Black Sea paleo-oceanic lithospheric plate (i.e. the remnants of the ancient Tethys ocean) (Fig. 2) in its eastern sector (Eastern Pontides) under the East-European lithospheric paleo-continental plate. Spatial distribution of the basic shaft-like tectonic structures in the East Black Sea paleo-oceanic basin and adjacent territories (Great and Minor Caucasus, formerly being the parts of this basin) allow regarding the tectonic structure of the East Black Sea basin (and spatial position of its zone of subduction) as having undergone inconsiderable changes during the last 65 m.y. (Fig. 2, maps № 3 – № 6). Consequently, the relict geodynamical processes and rheological parameters of interiors in the Tethys paleo-oceanic plate (the ancient Mediterranean-East Black Sea paleo-subduction region) can be modeled on the basis of available geological and geophysical data (Fig. 3).

COMPUTATION OF PARAMETERS OF THE GEODYNAMICAL MODEL OF THE MEDITERRANEAN-EAST BLACK SEA SUBDUCTION ZONE

Geodynamical model of the thermo-mechanical state of the mantle wedge between the base of the East-European lithospheric platform and the upper surface of the Mediterranean-East Black Sea paleo-oceanic lithospheric plate, subducting at the angle β with the velocity V, is constructed as a solution of the 2D infinite Prandtl number ($\mathrm{Pr} \to \infty$) non-dimensional hydrodynamic equations for the stream function ψ and temperature T in the Boussinesq approximation (Schubert et al., 2001):

$$(\partial^2_{zz} - \partial^2_{xx}) \times \eta \times (\partial^2_{zz} - \partial^2_{xx}) \times \psi + 4 \times \partial^2_{xz} \eta \times \partial^2_{xz} \psi = Ra \times T_x - Ra^{(410)} \times \Gamma_x^{(410)} - Ra^{(660)} \times \Gamma_x^{(660)}, \quad (1)$$

$$\partial_t T = \Delta T - (\psi_z \times T_x) + (\psi_x \times T_z) + ' + (Di / Ra) \times (\tau^2_{ik} / 2 \times \eta) + Q, \quad (2)$$

Here η is dynamic viscosity, ∂ and indices denote partial derivatives with respect to coordinates x (horizontal), z (vertical) and time t, Δ is the Laplace operator, $\Gamma_x^{(410)}$ and $\Gamma_x^{(660)}$ are volumetric ratios of the heavy phase at the 410 km and 660 km phase boundaries i.e. the step functions with a blurred (not sharp) upper boundaries, reflecting gradual increase of volumetric ratio of a heavy phase, the velocity components V_x and V_z are expressed through ψ as (x-axis is pointing opposite to the subduction direction along the base of the mantle transition zone (MTZ) at the depth of 660 km, z-axis is pointing upwards from MTZ). Equations (1) – (2) allow calculating finite-amplitude convection, in contrast to the case of infinitesimal convective perturbations, exponentially growing in time t according to the law $\exp(\gamma(x) \times t)$ within the framework of the problem of onset of convection, where $\gamma(x)$ is the growth rate.

$$V_x = \psi_z, \quad V_z = -\psi_x, \quad (3)$$

while non-dimensional Rayleigh number Ra, phase numbers; $Ra^{(410)}$, $Ra^{(660)}$ and dissipative number Di are

$Ra = [(\alpha \times \rho \times g \times d^3 \times T_1) / (\eta_C \times \chi)] = 5.55 \times 10^8$;
$Ra^{(410)} = [(\delta\rho^{(410)} \times g \times d^3) / (\eta_C \times \chi)] = 6.60 \times 10^8$;

$$Ra^{(660)} = [(\delta\rho^{(660)} \times g \times d^3) / (\eta_C \times \chi)] = 8.50\times10^8;\ Di = [(\alpha \times g \times d) / c_p] = 0.165, \quad (4)$$

where $\alpha = 3\times10^{-5}$ K^{-1} is the thermal expansion coefficient, $\rho = 3.3$ g·cm^{-3} is the density, g is gravity acceleration, $c_p = 1.2\times10^3$ J · kg^{-1}·K^{-1} is specific heat capacity at constant pressure, $T_1 = 1950^o$ K is the temperature at the base of the mantle transition zone (MTZ) at the depth of 660 km regarded as the lower boundary of the model domain, $Q = 6.25\times10^{-4}$ mW·m^{-3} is the volumetric heat generation in the crust, τ_{ik} is the viscous stress tensor, $d = 660$ km is the vertical dimension of the modeled domain, $\eta_C = 10^{18}$ Pa · s is the viscosity scaling factor, $\chi = 1$ mm^2 · s^{-1} is thermal diffusivity, $\delta\rho^{(410)} = 0.07\rho$ and $\delta\rho^{(660)} = 0.09\rho$ are the density changes at the 410 km and 660 km phase boundaries respectively. In (1), (2) the scaling factors for time t, coordinates x and z, stresses τ_{ik}, and the stream-function ψ are ($d^2 \times \chi^{-1}$), d, ($d^{-2}\times\eta_C \times \chi$) and χ respectively. Assuming rheology be nonlinear for the dislocation creep deformation mechanism dominating in the mantle wedge, saturated with water, expelled from the subducting slab, we accept the temperature-, stress-, and lithostatic pressure p dependent viscosity as (Zharkov, 2019)

$$\eta = (1 / 2 \times A \times C_w^r \times \tau^{n-1}) \times (h / b^*)^m \times \{\exp [(E^* + p\times V^*) / (R \times T)] \}, \quad (5)$$

where T is the absolute temperature. According to Trubitsyn (2014), for "wet" olivine $n = 3$, $r = 1.2$, $m = 0$, $\tau = (\tau_{ik}^2)^{1/2}$, $E^* = 480$ (kJ ×mol^{-1}), $V^* = 11\times10^3$ (mm^3 ×mol^{-1}), $A = 10^2$ s^{-1}×(MPa)$^{-n}$, $C_w > 10^{-3}$ for "wet" olivine is weight water content(in %%) (Hirschmann, 2006). At $C_w = 10^{-3}$ on account of

$$\tau_{ik}^2 = (4 \times \eta^2) \times [(\psi_{zz} - \psi_{xx})^2 / 2 + 2 \times \psi_{xz}^2], \quad (6)$$

non-dimensional viscosity is

$$\eta = \{ 1.0 / [(\psi_{zz} - \psi_{xx})^2 / 2 + 2 \times \psi_{xz}^2]^{1/3}\} \times \exp \{[10.0 + 5.0 \times (1 - z)] / T\} \quad (7)$$

The aspect ratio of the modeled domain is accepted equal to 1: (1.85) so that for the subduction along the diagonal the angle of subduction is $\beta = 28°$ while the trial velocity $V = 40.5$ mm×y^{-1} scaled by ($d^{-1}\times \chi$) equals $V = 0.938\times10^3$, i.e. in the subducting East Black Sea paleo-oceanic plate (the Tethys paleo-oceanic plate) the velocity components are $V_x = -0.898\times10^3$ и $V_z = -0.268\times10^3$ (Finetti, 1988). The trial subduction velocity is selected to provide the 2D convection in the mantle wedge to be aroused with the cell dimension ~ 250 km (as judged about by the nearly identical separation between the adjacent shaft-like orogenic structures in the paleo-ocean Tethys in Figure 2, maps № 3 – № 6, existed since the Late Cretaceous (65 m.y.) till present).

Following Trubitsyn (2014) the phase functions $\Gamma^{(l)}$ are taken as (it should be kept in mind that z-axis here is pointing upwards, and thus the signs are changed):

$$\Gamma^{(l)} = (1 / 2) \times \{1 - th [z - z^{(l)}(T)] / w^{(l)}\};\ z^{(l)}(T) = z_o^{(l)} - \{[\gamma^{(l)} \times (T - T_o^{(l)})] / (\rho \times g)\}, \quad (8)$$

where $z^{(l)}(T)$ is the depth of the l-th phase transition. $z_0^{(l)}$ and $T_0^{(l)}$ are the averaged depth and temperature of phase transition, $\gamma^{(410)} = 3$ (MPa×K^{-1}) and $\gamma^{(660)} = -3$ (MPa×K^{-1}) are the slopes of the phase equilibrium curves, $w^{(l)}$ is the characteristic thickness of the l-th phase transition, $T_0^{(410)} = 1800^o$ K, $T_0^{(660)} = 1950^o$ K are the mean phase transition temperatures. The heats of phase transitions are neglected in (2) as insignificant in the case of developed convection as in (Trubitsyn and Trubitsyn, 2014). From (8) it follows

$$\Gamma_x^{(l)} = -(\gamma^{(l)} / 2 \times \rho \times g \times w^{(l)}) \times T_x \times ch^{-2}\{[(z - z_o^{(l)} + \gamma^{(l)} \times (T - T_o^{(l)})) / (\rho \times g)] / w^{(l)}\}, \quad (9)$$

where from it is clear that the phase transitions with $\gamma^{(l)} > 0$ facilitate convection (at $l = 410$), while the phase transitions with $\gamma^{(l)} < 0$ (at $l = 660$) suppress it. In the dimensionless form $z_0^{(410)} = 0.38$, $z_0^{(660)} = 0$, $w^{(l)} = 0.05$, $\gamma^{(410)} = 2.55\times10^9$, $\gamma^{(660)} = -2.55\times10^9$, $T_0^{(410)} = 0.92$, $T_0^{(660)} = 1.00$, and in (1)

$$\Gamma_x^{(l)} = -(\delta\rho^{(l)} \times \gamma^{(l)} / 2\times\rho\times Ra^{(l)}\times w^{(l)}) \times T_x \times ch^{-2}\{[z - z_o^{(l)} + \gamma^{(l)} \times (\delta\rho^{(l)}/\rho \times Ra^{(l)})\times(T - T_o^{(l)})]/w^{(l)}\}, \quad (10)$$

Equations (1)–(2) are solved for the isothermal horizontal and insolated vertical boundaries regarded no-slip impenetrable ones except for the "windows" for in- and outgoing subducting plate, where the plate velocity is specified. Vertical boundary distant from subduction zone is assumed penetrable at right angle, which angle does not differ greatly from the angle at which this boundary is crossed in the case of very flat subduction. Q in (2) is non-zero in the continental and oceanic crust 40 km and 7 km thick. Initial vertical boundaries temperature is calculated for the half-space cooling model for 10^9 yr and 10^8 yr for the East-European (continental) and Mediterranean-East Black Sea (oceanic) plates respectively.

RESULTS OF COMPUTATION OF GEODYNAMICAL PARAMETERS IN THE ZONE OF SUBDUCTION

Initial estimate of the mean velocity of subduction of the Mediterranean-East Black Sea lithospheric plate can be obtained via the dependence of the convective 2D instability growth rate $\gamma(x)$ on the horizontal coordinate x for convection having the form of tectonic shaft-like structures aligned across the direction of subduction within

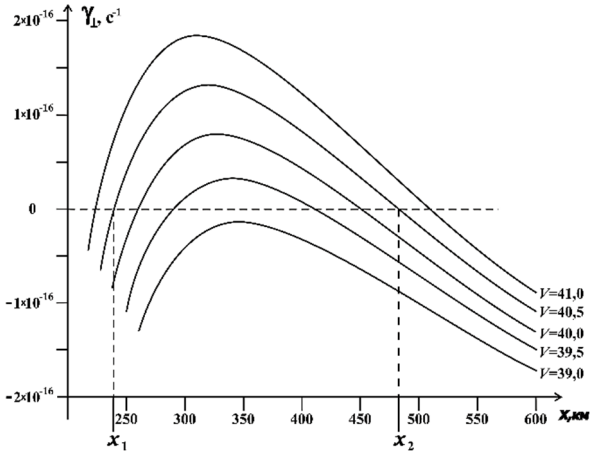

Fig. 4 Growth rate $\gamma(x)$ of convective instability vs. horizontal distance x, for subduction velocities V in mm per year. In the zone ($x_1 < x < x_2$), approximately 250 km long, single 2D convection cell with $\gamma(x) > 0$ is aroused at $V = 40.5$ mm×yr^{-1} in the zone of heat flux maximum.

the framework of the constant viscosity fluid model. However, the model temperature- and pressure viscosity dependence is taken into account in the averaged manner, see the exponential factor, describing the T-, p-dependence of viscosity, is considered to be equal to its mean value. Growth rates $\gamma(x)$, calculated with the analytical formulae in (Gavrilov, 2014), are shown in Figure 4 for the subduction angle $\beta = 28°$, convection cell dimension of 230-470 km, and subduction velocity V given in Figure 4 in mm×yr^{-1}.

It should be underlined that $\gamma(x)$ is viscosity-independent since the convection driving force is the dissipative heating directly proportional to viscosity, while, on the other hand, the greater the viscosity the more difficult is to arouse the convection. Figure 4 demonstrates the convective zone with $\gamma(x) > 0$ to amount to $x_2 - x_1 = 250$ km in size (i.e. the 250 km long convective cell is actually aroused) at the subduction velocity $V = 40.5$ mm per year which can be regarded as the initial trial velocity estimate.

To construct the consistent more accurate model of small-scale thermal convection in the mantle wedge between the overriding East-European platform and subducting East Black Sea paleo-oceanic lithospheric plate it is necessary, first, to set $Ra = 0$, $Di = 0$ in (1)-(2) to obtain the more precise model of thermo-mechanical state of subducting slab, mantle wedge and overriding plate without viscous dissipation and convection. Such the approach is associated with that with Ra and Di (4) convection undergoes stages with high convective velocities thus requiring extremely small time steps to reach the quasi stationary state. Integrating (1) – (2) with $Ra \to 0$, $Di = 0$, i.e. by means of finite-element method on the grid 104×104 in space and the 3-rd order Runge-Kutta method in time with $V = 40.5$ mm per year one

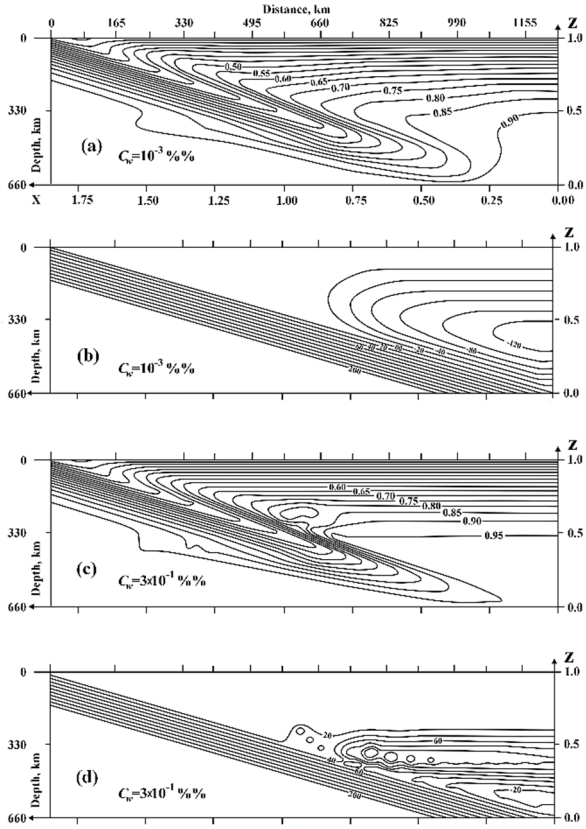

Fig. 5 Quasi steady-state non-dimensional stream-function (ψ) and temperature (T) distributions along the profile MB in the zone of subduction of the Tethys paleo-oceanic plate (Mediterranean-East Black Sea lithospheric paleo-oceanic plate) under the lithosphere of East European paleo-continental plate, with no effects of dissipative heating and convection taken into account for non-Newtonian rheology: (a, b) for the water content in rocks $C_w = 10^{-3}$ weight %% and (c, d) for the water content in rocks $C_w = 3\times10^{-1}$ weight %%. Parallel equidistant streamlines represent subducting Mediterranean-East Black Sea plates, the streamlines above correspond to the mantle wedge flow induced by subduction.

obtains quasi stationary model ψ and $T - T_R$ distributions (accounting for heat conduction and advection) shown in Figure 5 with the streamlines and isotherms shown with the 0.25 and 0.05 intervals.

Figure 5 shows the results of computation for non-Newtonian rheology (formulae (7) – (9) for viscosity), in Figure 5 (a, b) for the water content $C_w = 10^{-3}$ weight %% in the mantle wedge rocks, and in Figure 5 (c, d) for $C_w = 3\times10^{-1}$ weight %%. The velocity $V = 40.5$ mm per year is chosen to provide the best fit to the observed heat flux distribution. The Mediterranean-East Black Sea lithospheric paleo-oceanic plate subducting with a given velocity V (shown by the equidistant diagonal streamlines) is considered rigid. The viscosity in the zone of friction between the lithospheric plates at temperatures below 1200 °K is reduced by two orders of magnitude in

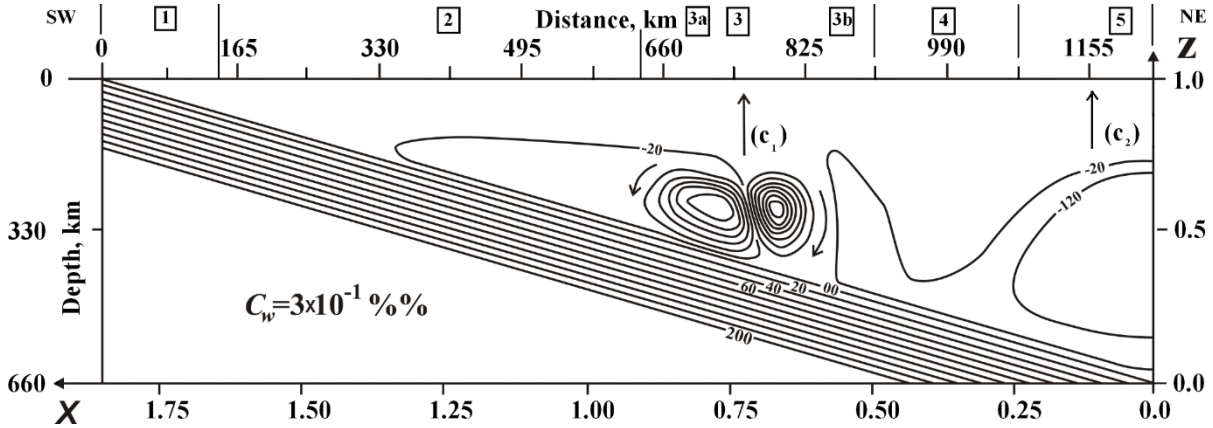

Fig. 6 Quasi steady-state stream-function in the mantle subduction wedge along the profile MB of the Mediterranean-East Black Sea paleo-oceanic plate (the Tethys paleo-oceanic plate) under the lithosphere of East European paleo-continental plate (Caucasus region), with the effects of dissipative heating and convective instability for the case of non-Newtonian rheology and the water content C_w =3×10^{-1} weight %%. Arrow (C_1) and (C_2) shows ascending convective flow transporting calc-alkali magmas (with the metals which are contained in them) at the point C_1 (Archangelsky (3a) and Schatsky (3b) uplifts) and at the point C_2 (Great Caucasus region). 1 – the Mediterranean region; 2 – the peninsula of Asia Minor (Eastern Pontides); 3 – the East Black Sea depression; 3a0 – the Archangelsky uplift zone; 3b – the Schatsky uplift zone; 4 – the Great Caucasus region; 5 – the Indolo-Kubansky depression.

comparison with (5) to take into account the effect of lubrication due to partially entrained subducting deposits which prevent gluing to the overriding lithosphere (Geria, 2011). Comparing Figures 4b and 4d shows the return flow to be induced as a single vortex at C_w = 10^{-3} weight %% and as the two horizontally shifted vortices (located one above another) at C_w = 3×10^{-1} weight %%, these two vortices being substantially vertically compressed and the upper (with $\psi > 0$) rotating clockwise while the lower (with $\psi < 0$) – counterclockwise. Micro-whirls ~ 10^2 km large between the oppositely moving layers inside the upper induced flow obviously owe their origin to the tangential discontinuity instability (Kelvin-Helmholtzian instability).

Setting the *Ra* and *Di* parameters in (1) – (2) according to (4), i.e. switching on the effects of dissipation and convection, and integrating (1) – (2), one finds out the convection not to be aroused at C_w = 10^{-3} weight %% and to be aroused and to destroy the induced mantle flow at C_w = 3×10^{-1} weight %% the convection during the non-dimensional time 0.6×10^{-6} (in dimensional form ~10^5 yr) having assumed the quasi steady-state form shown in Figure 6. Vorticose streamlines shown with the interval 4×10^4 are seen to actually correspond to a single convective cell aroused at the velocity of subduction V = 40.5 mm×yr^{-1}. It is worth emphasizing that the dimension of the Karig-Richter convective cell is of the order of 250 km.

Thus the computation with the non-Newtonian viscosity given by (7) – (9) shows the reduction of viscosity by the three orders of magnitude in comparison with (7) – (9) (i.e. at C_w = 3×10^{-1} weight %%) the convection is developed in the form of two micro-whirls capable to provide the 2D anomalous heat flux. Alternatively, the mantle wedge water content may be increased by less than to C_w = 3×10^{-1} weight %%, but the energy of activation be reduced (or constant A be increased) as compared to corresponding values given in (Trubitsyn, 2014). Considerable velocities of convective motions are due to the local viscosity reduction because of stress concentration in the zone of convection in the mantle.

The results of computations are shown in Figure 6, in which the quasi steady-state non-dimensional stream-function is depicted in the mantle subduction wedge with a sharp angle characteristic of subduction of the Mediterranean-East Black Sea paleo-oceanic plates (the Tethys paleo-oceanic plate) under the East-European continental platform.

The transversal roll-like structures are as well established not to originate at the angle of subduction $\beta > 30°$ above the subducting and Mediterranean-East Black Sea paleo-oceanic plate ((the Tethys paleo-oceanic plate)) (Geria, 2011; Gavrilov, 2014). At the angle of subduction $\beta = 28°$ under consideration the convection does not appear at the subduction velocity below V = 40.5 mm×yr^{-1}. It is obvious that the 2D convection in the narrow mantle wedge is associated with the greater viscous stresses (and consequently greater dissipative heating) than in the wider mantle wedge. In the case of non-Newtonian rheology mantle convection is aroused at the subduction velocity V = 40.5 mm×yr^{-1} at the water content C_w = 3×10^{-1} weight %%.

RESULTS AND DISCUSSION

The results of present research show the lasting (for 165 Myr) geodynamic and tectonic processes of subduction of the East Black Sea paleo-oceanic plate to result in formation of alternating parallel to each

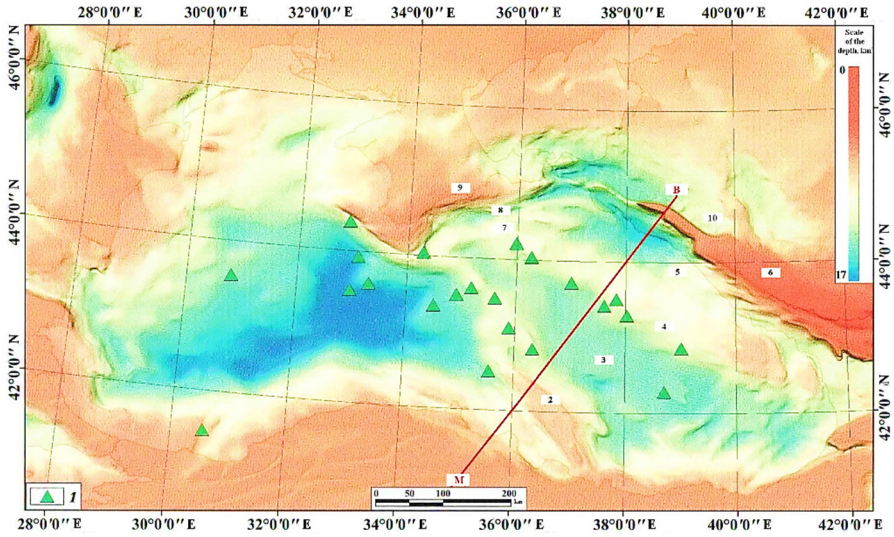

Fig. 7 Map of the relief of the hard surface of the Earth of the Black Sea and Azov Sea region (Glumov et al., 2014). 1 –green triangles indicate the lineal areas of discharge of gas and hydro fluid flows on the sea floor in the zones of rise of calcareous-alkaline magmas along deep tectonic faults; 2 – linearly elongated Archangelsky tectonic uplift structure; 3 – linearly elongated trough of the sea bottom surface relief associated with the depression of the East Black Sea basin; 4 – the Schatsky tectonic uplift structure; 5 – the Tuapse depression; 6 – linearly elongated uplift orogenic region of the Great Caucasus ; 7 – the Sorokin tectonic uplift structure; 8 – the pre–Crimean depression; 9 – the Crimean orogenic region; 10 – the Indolo-Kubansky depression. MB – the profile of the geodynamic model of the Mediterranean-East Black Sea subduction zone.

other linear uplifts (the Archangelsky uplift (2) and Schatsky uplift (4)) and the linear deep-sea stretched depressions (the depression of the East Black Sea basin (3) and the Tuapse depression (5)) in front of the orogenic region of the Great Caucasus (6) and the Sorokin uplift (7), the pre-Crimean depression (8), the Crimean orogenic region (9), represented on the map of the solid Earth relief in the Black and Azov Sea region (Fig. 7).

These alternating linearly stretched uplifts and depressions are shown in the temporary seismic section (Fig. 8) across the eastern part of the East Black Sea aquatic territory (the inset in the lower left corner of Fig. 8).

Figure 8 shows the Mohorovičić discontinuity (7), which may be regarded as the upper boundary of the East Black Sea lithospheric plate (in the lower right part of this seismic section), to have a definite northward slope under the orogenic roll-like tectonic structures of the Archangelsky uplift, the Schatsky uplift and Great Caucasus uplift. This slope indicates the East Black Sea plate to subduct under these orogenic structures during the current geochronological period. However, the velocity of subduction of the East Black Sea suboceanic plate remains so far indefinite and presently there are no pertinent published exact data on the subject.

According to (Geria et al., 2006; Geria, 2011; Gavrilov, 2014) there are two types of small-scale dissipation-driven mantle convection possible in the mantle wedge, viz. the 3D convection in the form of magma-carrying flows upwelling to the volcanic chains of the Archangelsky and Schatsky uplifts and located north of the East Black Sea depression, and the 2D convection in the form of transversal quasi-cylindrical Karig-Richter whirls (rolls) in the zones of Great Caucasus uplift and located north of the Indolo-Kubansky depression (Karig, 1971). In (Gavrilov, 2014) the spatial separation between these two types of thermal convection is shown to be due to temperature dependence of effective viscosity, the Karig-Richter whirls, if formed, being located somewhat behind the basic volcanic chain (Archangelsky and Schatsky – Minor Caucasus uplifts, Great Caucasus uplift).

Heat flux anomalies observed, e.g. in the central part of the East Black Sea depression (Kutas et al., 1993), owe their origin to the convective 3D convective heat supply respectively from the mantle wedge. The latter of these two heat flux maxima (i.e. the Indolo-Kubansky heat flux anomalies) is situated in the Great Caucasus is more pronounced (over the point C_2 in Figure 6) is of the 2D structure and apparently associated with the transversal rolls in the mantle wedge, while the former heat flux maximum (at the point C_1 coincident with the isolated concentric whirls of East Black Sea depression) is associated with the 3D convection (Fig. 9).

CONCLUSIONS

The results of the present modeling show that in carrying out the ore deposits prospecting-reconnaissance in the Caucasus region it is important to understand that the separation between the formed

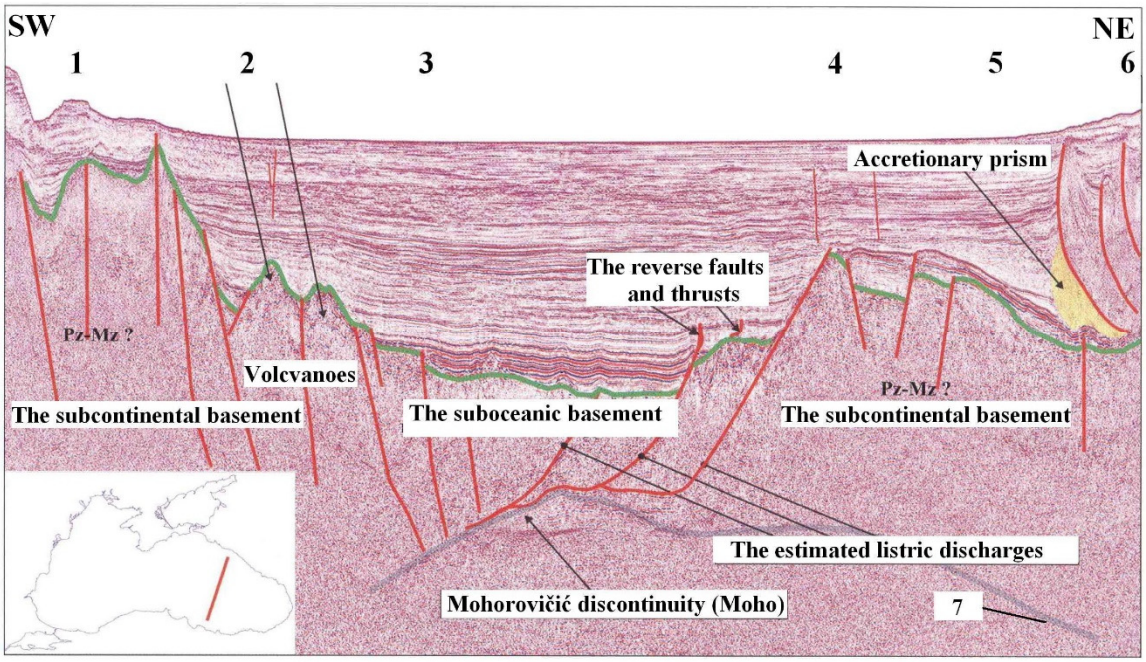

Fig. 8 Temporary seismic sounding section along the BC-060 profile (Glumov et al., 2014). 1 – the Archangelsky uplift; 2 – volcanic structures; 3 – the East Black Sea depression; 4 – the Schatsky uplift; 5 – the Tuapse depression; 6 - reset-shift structures; 7 - the line of the gray color indicates the Mohorovičić discontinuity (Moho) – the upper boundary of the subducting East Black Sea lithospheric oceanic plate; the line of the green color indicates the upper boundary of the consolidated continental and suboceanic basement; lines of the red color indicates the sub-vertical tectonic faults and associated listric discharges, which from the Mesozoic period to the present time were used to raise alkaline solutions, leading to the formation of metallogenic zones on the wave-like tectonic structures of the Black Sea and Azov Sea region.

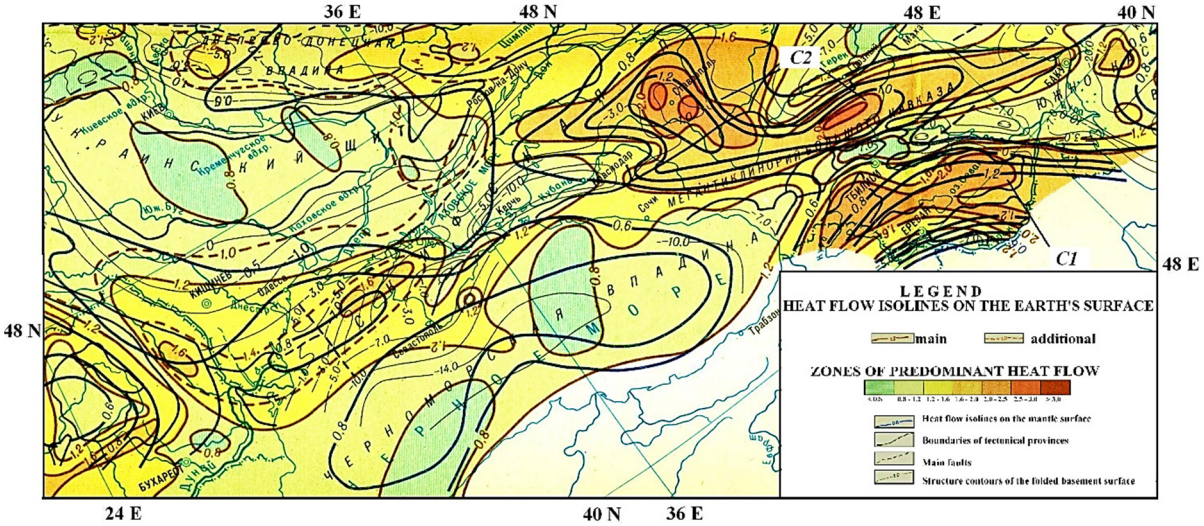

Fig. 9 The fragment of the map of value of heat flux q (I^{x} 41.8 mW / m^2) in the East Black Sea and Caucasus region (Smirnov, 1980). North of the Minor Caucasus (the Kumo-Manichsky depression) (C_1) and the Great Caucasus region (the Indolo-Kubansky depression) (C_2) are the zones of 3D and 2D convective flows ascending to the heat flux q maxima, the whirls under C_2 are the 2D Karig-Richter convective flows.

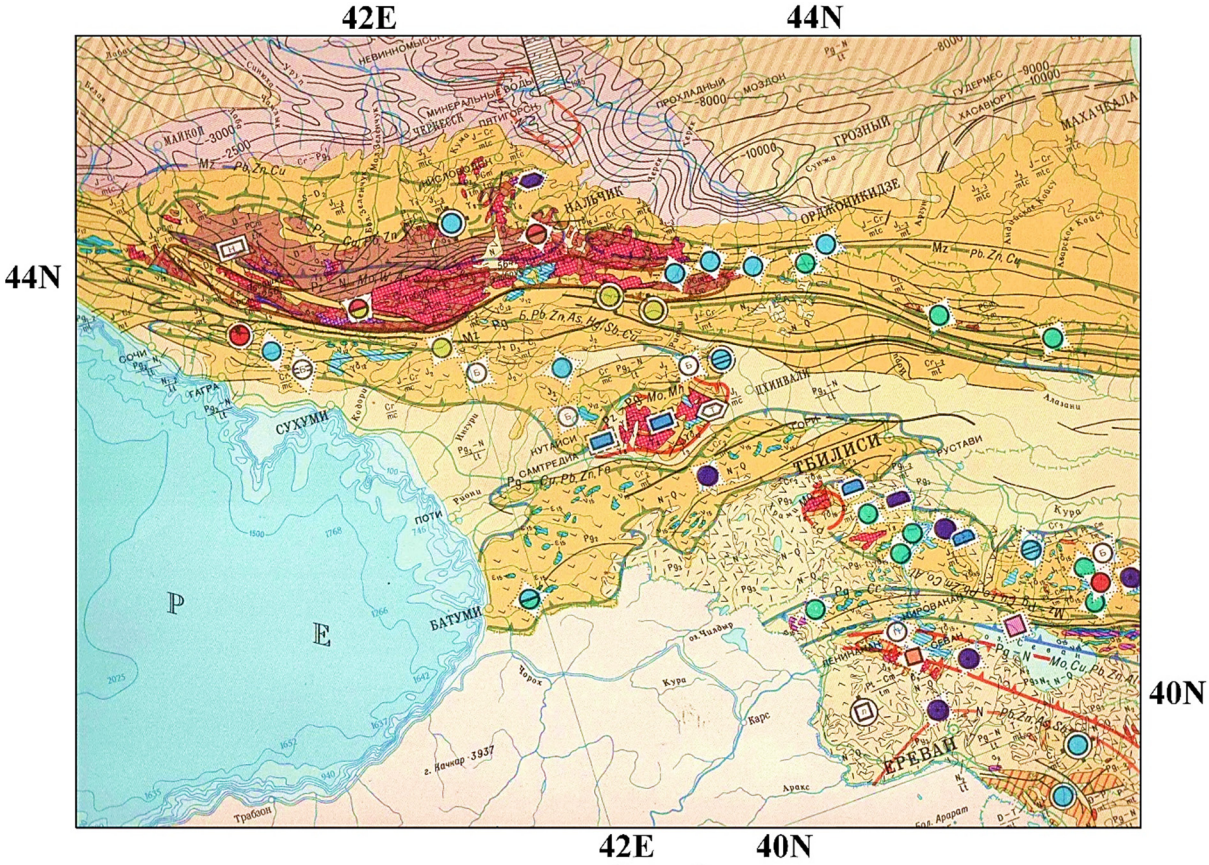

Fig. 10 The fragment of the map of mineral deposits in the territory of the Russian Federation (for the Caucasus region) (Kolosova, 1982). Black circle – iron (Fe) deposits; blue circle – copper (Cu) deposits; blue circle – different metal deposits (W, Mo, Pb, Zn et al.)

metallogenic provinces (zones) depends on many physical-chemical factors: angle of subduction and the velocity of subducting plate, temperature, pressure, viscosity, water content in the mantle wedge rocks, velocities of convective motion of the partially molten calc-alkali magmas in the Karig- Richter whirls, their dimensions as well as on other less significant rheological parameters of medium of the mantle wedge in the zone of subduction. For example, in the case of non-Newtonian rheology the characteristic dimension of convective cell of the Karig-Richter whirl in the model of mantle wedge over the Mediterranean-East Black Sea suboceanic lithospheric plate, subducting under the East-European continental lithospheric plate, amounts to ~ 300-400 km at the subduction velocity of 40.5 mm per year. This cell dimension is approximately coincident with the characteristic dimension of the 2D heat flux anomaly in the rear of the Great Caucasus. The mean water content in the mantle wedge is $C_w = 3\times10^{-1}$ weight %% (Hircshmann, 2006). The velocity of convective motions in the Karig-Richter whirls in this region exceeds 10 m per year which may be sufficient to provide efficient transport of calc-alcali magmas (along with metals solved in them) to the Earth's surface and contribute to formation of subsurface ore deposits. A sequential periodic distribution of the linearly elongated metallogenic provinces located with definite spatial intervals from the trench at the zone of subduction is reported in (Sillitoe, 1972). It is as well confirmed by the presence of the first chain ore deposits at the territory of Minor Caucasus, behind which the second chain of ore deposits is located at the territory of the Great Caucasus well seen in Figure 10.

Figure 10 shows the two linear nearly parallel roll-like tectonic zones of the ore deposits to locate in a distance of ~ 300 – 400 km at the territory of rolls of the Great and Minor Caucasus, which distance corresponds to the calculations given here. These linear roll-like zone of the Great and Minor Caucasus, along which the ore deposits are linearly distributed, are the continuations of roll-like zones located at the East Black Sea floor. For example, the Archangelsky and Schatsky rolls have its linear continuation at the territory of the mountain ridge (roll) of the Minor Caucasus. Formation of the ore deposits at the territory of Great and Minor Caucasus, Archangelsky and Schatsky rolls was contributed by the multiphase magmatic activity, volcanism, and ascent of alkali magmas with the dissolved metals. These magmas could have originated as a result of the pressure-release partial melting within the ascending

convective flows over the Karig-Richter whirls formed in the course of evolutionary geotectonic transformation of the East Black Sea region. Molten magma was ascending along the numerous cracks and faults in the rocks of the ridges of Caucasus. Bulky magmatic intrusions, originated above the centers of mantle convective whirls, intruded into the shale rocks, which were conserved thus far as the pegmatite lodes. Magmatic intrusions were effective the metamorphism in the zones of contact of the latter lodes with the ambient rocks thus having formed the quartz and quartz-carbonate veins with the poly-metallic ores. The biggest color metal deposit in the Caucasus is the Tyrnyauz wolfram-molybdenum ore belt associated with the zone of sub- latitudinal tectonic crust faults located along the ridges of Great Caucasus. Besides, the well-known copper ore deposit along the river Kesanta is also located within the 14 km wide sub-latitudinal band along the Caucasian ridge. Sub-latitudinal distribution of different parallel to each other poly-metallic ore deposits at the territories of Minor and Great Caucasus are ~ 300-400 km distant from each other, and such the separation confirms the results of present modeling, according to which ore deposits are linked with the sub-latitudinal quasi-cylindrical 2D и 3D convective Karig-Richter vortices aroused in the process of geological evolution in the zone of subduction of the Mediterranean-East Black Sea paleo-lithospheric plate (eastern part of the paleo-ocean Tethys).

REFERENCES:

Billen, M. and Hirth, G.: 2005, Newtonian versus non-Newtonian Upper Mantle Viscosity: Implications for Subduction Initiation. Geophys. Res. Lett., 32, L19304. DOI: 10.1029/2005GL023458

Condie, K.C.: 1976, Plate tectonics and crustal evolution. New York, Pergamon Press Inc., 288 pp.

Fercshtatter, G.B.: 2012, Paleozoic intrusive magmatism at Urals – a key to understanding the orogenesis nature. Litosfera, 1, 3–13, (in Russian).

Finetti, G.: 1988, Monograph on the Black Sea. Boll. Geofis. Teor. Appl., 30, 117–118.

Gavrilov, S.V.: 2014, Investigation of the island arc formation mechanism and the back-arc lithosphere spreading. Geofizicheskie Issledovaniya, 15, 4, 35–43, (in Russian).

Gavrilov, S.V. and Abbott, D.H.: 1999, Thermo-mechanical model of heat-and mass-transfer in the vicinity of subduction zone. Physics of the Earth, 35, 967–976, (in Russian).

Gerya, T.V.: 2011, Future directions in subduction modeling. J. Geodyn., 52, 344–378. DOI: 10.1016/j.jog.2011.06.005

Gerya, T.V., Connolly, J.A.D., Yuen, D.A., Gorczyk, W. and Capel, A.M.: 2006, Seismic implications of mantle wedge plumes. Phys. Earth Planet. Inter., 156, 59–74. DOI: 10.1016/j.pepi.2006.02.005

Glumov, I.F., Gulev, V.L., Senin, B.V. and Karnaukhov, S.M.: 2014, Regional geology and of the Black Sea deep depression and the shelf zones. Part 2, Moscow, Nedra Publishers, 181 pp., (in Russian).

Hirschmann, M.M.: 2006, Water, melting and the deep Earth H2O cycle. Ann. Rev. Earth Planet. Sci., 34, 629–653. DOI: 10.1146/annurev.earth.34.031405.125211

Hirth, G. and Kohlstedt, R.: 2003, Rheology of the upper mantle and the mantle wedge: A view from the experimentalists. In: Inside the Subduction Factory. Geophys. Monogr. Ser., 138, 83–105. DOI: 10.1029/138GM06

Isacks, B., Oliver, J. and Sykes, L.R.: 1968, Seismology and new global tectonics. J. Geophys. Res., 73, 5855–5900.

Karig, D.E.: 1971, Origin and development of marginal basins in the Western Pacific. J. Geophys. Res., 76, 11, 2542–2561. DOI: 10.1029/JB076i011p02542

Kolosova, L.N.: 1982, The map of mineral deposits in the territory of the USSR. Moscow, GUGK, (in Russian).

Kutas, R.I. and Tsviashenko, V.A.: 1993, Geothermal regime and seismicity of the Crimean peninsula. Geotermiya seysmichnih i aseysmichnih zon. Moscow, Nauka, 400 pp., (in Russian).

Noble, J.A.: 1970, Metal provinces and metal finding in the western United States. Bull. Geol. Soc. Am., 81, 1607–1624.

Schubert, G., Turcotte, D.L. and Olson, P.: 2001, Mantle Convection in the Earth and Planets. New York, Cambridge University Press, 940 pp. DOI: 10.1017/CBO9780511612879

Sillitoe, R.H.: 1972, Relation of metal provinces in Western America to subduction of oceanic lithosphere. Bull. Geol. Soc. Am., 83, 813–818.

Smirnov, Ya.B.: 1980, Heat flow map of the USSR and adjacent areas. Scale 1: 10 000 000. Moscow, GUGK, (in Russian).

Trubitsyn, V.P. and Trubitsyn, A.P.: 2014, Numerical model of formation of the set of lithospheric plates and their penetration through the 660 km boundary. Physics of the Earth, 6, 138–147, (in Russian).

Zharkov, V.N.: 2012, Physics of the Earth's Interiors. Moscow, Nauka i obrazovanie, 384 pp., (in Russian).